

## Density jumps across phase transitions in soft-matter systems

Hartmut Graf and Hartmut Löwen\*

*Institut für Theoretische Physik II, Heinrich-Heine-Universität Düsseldorf, Universitätsstraße 1, D-40225 Düsseldorf, Germany*

(Received 6 January 1998)

We investigate the magnitude of density jumps across phase transitions in soft-matter systems composed of macromolecular particles, like star polymers or colloidal suspensions. The standard route to predict phase transformations is to start from an effective interaction potential between these macroparticles and map the phase diagram onto that of the corresponding effective one-component system. Using density-functional perturbation theory, we demonstrate that this procedure leads to wrong density jumps if the number of microscopic degrees of freedom is coupled to the number of macroparticles. In particular, the microscopic degrees of freedom can drive a macroparticle phase transition to be *isochoric*, i.e., to occur without any jump in the macroparticle density. [S1063-651X(98)04005-7]

PACS number(s): 82.70.Dd

### I. INTRODUCTION

Mesoscopic soft-matter systems composed of supramolecular aggregates like colloids or star polymers represent excellent realizations of classical liquids on a mesoscopic length scale. By now, different colloidal suspensions can actually be well synthesized such that they consist of monodisperse spherical particles whose interaction can be modeled by a simple spherically symmetric effective pair potential  $V(R)$ ,  $R$  denoting the distance between the centers of two macromolecular particles [1]. The interesting point is that these colloidal spheres can serve as model systems to study phase transitions such as freezing, melting, and solid-to-solid transformations [2,3]. Recent research has focused on a detailed comparison between the experimental data of the phase diagram and theoretical calculations assuming a concrete form of  $V(R)$ .

A remarkable agreement was achieved for sterically stabilized colloids which are modeled as hairy balls described by a hard-sphere potential simply governed by excluded volume terms. In fact, experimental studies using samples of monodisperse polymethylmethacrylate (PMMA) spheres [4] reveal that the freezing transition perfectly coincides with that theoretically predicted from the hard-sphere model: there is a strong first-order freezing transition with a huge density jump of about 10% from a fluid into a face-centered-cubic crystal.

For charged colloidal suspensions the traditional linear screening theory of Derjaguin, Landau, Verwey, and Overbeek [5] is frequently invoked to describe the effective interparticle interactions. For index-matched suspensions this interaction assumes a Debye-Hückel (or Yukawa) form for  $V(R)$ . In fact by renormalizing the bare charge as dictated by nonlinear screening theory for strongly coupled systems [6], Monovoukas and Gast [7] could show that the experimental phase diagram of highly salted charge-stabilized polystyrene spheres could indeed be mapped onto that of a pure Yukawa system explored by computer simulation [8]. Less satisfactory agreement is achieved in the regime of deionized (salt-

free) charged suspensions where high accuracy scattering data for the liquid-solid phase boundaries are known [9].

Other interesting soft-matter systems exhibiting a rich phase behavior are polymeric micelles [10] and star polymers [11]. Here, calculations of the effective interactions are available [12] describing the experimental data [13] for the phase diagram [14].

In this paper we study the relation between the phase diagram of a soft-matter system and that of a one-component system interacting via the effective pair potential  $V(R)$  in more detail. Calculating phase boundaries means that one has to equate the total pressure and the chemical potential at fixed temperature. Hence the phase boundaries can strongly be affected by the huge number  $f$  of microscopic degrees of freedom which significantly contribute to the total pressure. If this number  $f$  is fixed by the number  $N_m$  of macroparticles, we show that the location of phase boundaries is significantly affected by the microscopic degrees of freedom. In this case, phase transitions can happen to be *isochoric* (i.e., there is no density jump). A linear relation between  $f$  and  $N_m$  is, for instance, established for star polymers with a fixed arm number or for salt-free charged suspensions where global charge neutrality couples the number of counterions to the number of macroions.

Our results are based on density-functional perturbation theory by which we obtain the effective potential together with additional contributions to the total free energy from the microscopic degrees of freedom. We first focus on a model of beads and springs for which the procedure is most transparent. This is then generalized towards a more realistic chain model of star polymers. Depending on the system parameters, we find that the correlational free energy of the monomers can dominate the total pressure. Then we use the density-functional language to describe linear screening theory for charged suspensions where we find that the entropic contributions of the counterions to the total pressure reduces any density jump across freezing considerably in the absence of salt. On the other hand, sterically stabilized suspensions and highly salted charged colloids exhibit density jumps across phase transformations.

Usually one performs a double tangent construction to get the coexisting densities in a plot of the isothermal free energies per particle versus inverse density. Our analysis shows

\*Also at Institut für Festkörperforschung, Forschungszentrum Jülich, D-52425 Jülich, Germany.

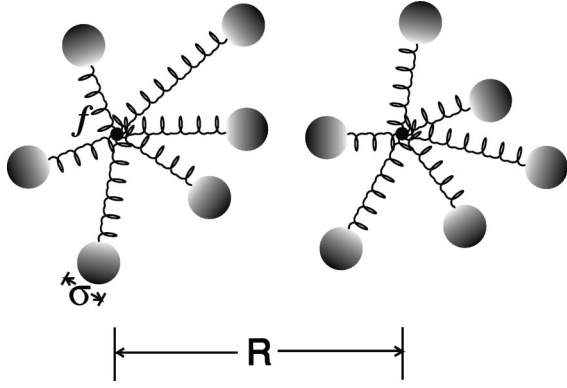


FIG. 1. Schematic picture of the bead-spring model used.  $f$  springs carrying hard spheres of diameter  $\sigma$  are attached to a small central core. The core-core separation is  $R$ .

that the microscopic degrees of freedom may change the situation insofar as one has simply to take the minimum of the free energies in the effective one-component system. Hence phases in the effective one-component model that are metastable and preempted by a density jump of other phase transitions can now turn out to be thermodynamically stable soft-matter phases.

Although our arguments are simple, the results have apparently not been stated for soft-matter systems, apart from very recent papers by van Roij and co-workers [15,16]. The importance of the microscopic degrees of freedom in soft-matter systems was already pointed out by Silbert and co-workers [17,18] but the implication on phase transitions was not discussed there. In the case of charged suspensions, the osmotic pressure was recently obtained together with the counterionic contributions in Ref. [19] but its influence on density jumps across phase transitions was not discussed there. We finally remark that there is also an analog to liquid metals where the electrons play the role of microscopic degrees of freedom [20].

Our paper is organized as follows: First we introduce a bead-spring model for a star polymer in Sec. II. Using density-functional perturbation theory we show that the effective interaction potential  $V(R)$  is Gaussian. Calculating the freezing transition we demonstrate that the number  $f$  of microscopic degrees of freedom in fact reduces the density jump across freezing. Then, in Sec. III, we generalize our result to star polymers. The linear screening theory of salted suspensions with an effective Yukawa pair potential is discussed extensively in Sec. IV. We finally conclude in Sec. V.

## II. BEAD-SPRING MODEL FOR SUPRAMOLECULAR AGGREGATES

### A. Definition of the model

In order to demonstrate clearly the interplay between the microscopic and mesoscopic degrees of freedom for a colloidal phase transition let us introduce and discuss a simple bead-spring model. The centers of a supramolecular particle are modeled as pointlike cores where  $f$  microscopic springs are attached. Each spring carries one hard sphere of diameter  $\sigma$  at its other end, see Fig. 1. Hence the potential energy of a hard sphere at position  $\vec{r}$  attached to its core at position  $\vec{R}$  is

$$U(|\vec{r}-\vec{R}|) = K(\vec{r}-\vec{R})^2/2, \quad (1)$$

where  $K$  is the spring constant. We assume  $f \gg 1$  in the following. An analytical treatment of the effective interactions becomes possible if the hard spheres do not interact with each other, or—formally—if the diameter  $\sigma$  vanishes. Then the number density profile  $\rho(\vec{r})$  of the hard spheres around a single core centered at position  $\vec{R}$  is readily calculated to be

$$\rho(\vec{r}) = f \left( \frac{\beta K}{2\pi} \right)^{3/2} \exp[-\beta K(\vec{r}-\vec{R})^2/2] \equiv \phi(|\vec{r}-\vec{R}|), \quad (2)$$

where  $\beta \equiv 1/k_B T$  is the inverse thermal energy and  $\phi(r)$  has the meaning of a density orbital function. The typical extension of the density profiles is contained in the length scale  $a = \sqrt{k_B T/K}$ . The corresponding canonical free energy of the harmonically coupled indistinguishable beads is

$$F_0 = \frac{f}{\beta} \ln \left[ \Lambda^3 f \left( \frac{\beta K}{2\pi} \right)^{3/2} \right], \quad (3)$$

where  $\Lambda$  is the thermal de Broglie wavelength of the spheres.

### B. Density-functional perturbation theory of the effective interaction

Let us first note that the result from Sec. II A can alternatively be obtained by minimizing the free energy density functional

$$\begin{aligned} \mathcal{F}_0([\rho(\vec{r})], \vec{R}) &= \frac{1}{\beta} \int_{\mathcal{V}} d^3 r \rho(\vec{r}) \{ \ln[\Lambda^3 \rho(\vec{r})] - 1 \} \\ &+ \int_{\mathcal{V}} d^3 r \rho(\vec{r}) U(|\vec{r}-\vec{R}|) \end{aligned} \quad (4)$$

with respect to  $\rho(\vec{r})$  under the constraint of fixed average density

$$\int_{\mathcal{V}} d^3 r \rho(\vec{r}) = f, \quad (5)$$

where  $\mathcal{V}$  is the system volume. Inserting the result into the functional yields again the corresponding free energy (3).

The next step is to consider  $N_m$  macroparticles (i.e., cores) located at positions  $\{\vec{R}_1, \dots, \vec{R}_{N_m}\}$  each of them carrying  $f$  noninteracting beads. The total density profile is then a linear superposition of density orbitals  $\phi$  centered at the macroparticle positions. This result can be obtained again by minimizing the free energy functional

$$\begin{aligned} \mathcal{F}_0([\{\rho_i(\vec{r})\}], \{\vec{R}_1, \dots, \vec{R}_{N_m}\}) \\ := \sum_{i=1}^{N_m} \mathcal{F}_0([\rho_i(\vec{r})], \vec{R}_i) \end{aligned} \quad (6)$$

with respect to  $\{\rho_i(\vec{r}), \dots, \rho_{N_m}(\vec{r})\}$  under the constraint

$$\int_{\mathcal{V}} d^3 r \rho_i(\vec{r}) = f, \quad i = 1, \dots, N_m. \quad (7)$$

Here,  $\rho_i(\vec{r})$  is the density of spheres centered around particle  $i$ . The total free energy is  $N_m F_0$ .

We now perturb the system by considering also the hard-sphere interaction among the beads. For weak local packing fractions, the leading contribution can be written in the local density approximation by adding the term

$$\mathcal{F}_{\text{int}} \equiv \int_{\mathcal{V}} d^3r \Psi(\rho_{\text{tot}}(\vec{r})) \quad (8)$$

to the functional  $\mathcal{F}_0[\{\rho_1(\vec{r}), \dots, \rho_{N_m}(\vec{r})\}]$  where  $\Psi(\rho)$  is the excess free energy per unit volume of a uniform hard-sphere fluid and  $\rho_{\text{tot}}(\vec{r}) = \sum_{i=1}^{N_m} \rho_i(\vec{r})$  is the total number density of the spheres. An analytical expression for  $\Psi(\rho)$  is provided within the Carnahan-Starling approximation [21]

$$\Psi(\rho) = \frac{1}{\beta} \rho \frac{\eta(4-3\eta)}{(1-\eta)^2}, \quad (9)$$

where  $\eta = \pi\rho\sigma^3/6$  is the packing fraction.

As a further approximation, we expand the additional contribution (8) and (9) quadratically around the mean hard-sphere density  $\bar{\rho} \equiv f\rho_m$  where  $\rho_m = N_m/V$  is the mean number density of the macroparticles, i.e.,

$$\begin{aligned} \Psi(\rho_{\text{tot}}(\vec{r})) &= \Psi(\bar{\rho}) + \frac{d\Psi(\bar{\rho})}{d\rho} [\rho_{\text{tot}}(\vec{r}) - \bar{\rho}] \\ &+ \frac{1}{2} \frac{d^2\Psi(\bar{\rho})}{d\rho^2} [\rho_{\text{tot}}(\vec{r}) - \bar{\rho}]^2 + \dots \end{aligned} \quad (10)$$

In first-order perturbation theory the total free energy is that of the unperturbed system  $N_m F_0$  plus the perturbation (8) evaluated at the unperturbed density fields. This finally yields for the total microparticle-averaged free energy

$$F_{\text{mic}} = F_1 + F_2, \quad (11)$$

with four different terms which depend on the core density but not on the core configuration:

$$\begin{aligned} F_1 &= \frac{1}{\beta} \ln \left[ \Lambda^3 f \left( \frac{\beta K}{2\pi} \right)^{3/2} \right] \bar{\rho} \mathcal{V} + \Psi(\bar{\rho}) \mathcal{V} - \frac{1}{2} \frac{d^2\Psi(\bar{\rho})}{d\rho^2} \bar{\rho}^2 \mathcal{V} \\ &+ \frac{1}{16} \frac{d^2\Psi(\bar{\rho})}{d\rho^2} \bar{\rho} f \left( \frac{\beta K}{\pi} \right)^{3/2} \mathcal{V}. \end{aligned} \quad (12)$$

These terms are frequently called ‘‘volume terms’’ [20,17] since they directly scale with the system volume  $\mathcal{V}$ . Furthermore the effective potential energy is contained in  $F_2$ , i.e.,

$$F_2 = \frac{1}{2} \sum_{\substack{i,j \\ i \neq j}}^{N_m} V(|\vec{R}_i - \vec{R}_j|). \quad (13)$$

The effective pair potential  $V(R)$  is Gaussian and given by a convolution of two density orbitals

$$\begin{aligned} V(R) &= \frac{d^2\Psi(\bar{\rho})}{d\rho^2} \int_{\mathcal{V}} d^3r \phi(|\vec{r} - \vec{R}|) \phi(r) \\ &= \frac{1}{8} \frac{d^2\Psi(\bar{\rho})}{d\rho^2} f^2 \left( \frac{\beta K}{\pi} \right)^{3/2} \exp(-\beta K R^2/4). \end{aligned} \quad (14)$$

Note that the effective potential depends both on the macroparticle density  $\rho_m$  and on temperature  $1/\beta$ .

Let us finally discuss the relative importance of the four different ‘‘volume terms’’ in Eq. (12): the first one does not affect the location of phase boundaries since it simply shifts the free energy per core by a constant in both phases. If the density  $\bar{\rho}$  is small, the function  $\Psi(\bar{\rho})$  is practically quadratic in  $\bar{\rho}$ , and hence the second and the third ‘‘volume term’’ cancel each other. The most important contribution is the remaining fourth term which describes the density-dependent correlation energy of a single star. It is this density dependence that will significantly affect the location of phase boundaries.

### C. The freezing transition of a Gaussian potential

Up to now we have not yet considered the canonical average of the macroparticles. In fact, the total free energy gained in the last section only concerns an average over the microscopic degrees of freedom and is the pure potential energy as far as the macroparticles are concerned. The total effective Hamiltonian  $\mathcal{H}_{\text{eff}}$  of the macroparticles

$$\mathcal{H}_{\text{eff}} = K_m + F_1 + F_2 \quad (15)$$

involves the kinetic energy  $K_m$  of the macroparticles plus their total potential energy (11). It is this effective Hamiltonian which has to be canonically averaged with respect to the macroparticle coordinates  $\{\vec{R}_i\}$ . Thus we obtain the total canonical free energy as

$$F = F_1 + F_3, \quad (16)$$

where  $F_3$  is the Helmholtz free energy of a classical system interacting via Gaussian pair potentials for fixed temperature and core number density  $\rho_m \equiv N_m/V$ . Now the crucial point is that one has not to forget the ‘‘volume term’’  $F_1$  [22].

We are interested in the region of low temperature and moderate density  $\rho_m$  where the system behaves as an effective hard-sphere system of macroparticles and freezes from a disordered fluid into a face-centered cubic crystal. We use a mapping onto a hard-sphere reference system as proposed and used by Barker and Henderson [23] to estimate the free energies  $F_3$  of the ‘‘Gaussian’’ fluid and solid. This procedure is defined as follows: We introduce an auxiliary core diameter  $d$  via

$$d = \int_0^\infty dR \{1 - \exp[-\beta V(R)]\} \quad (17)$$

and approximate the free energy of the *fluid* by the Carnahan-Starling free energy [21] of the corresponding hard-sphere system which is explicitly given by

$$F_3 \equiv F_3^f = F_3^{\text{id}} + F_3^{\text{CS}}, \quad (18)$$

where

$$F_3^{\text{id}} = k_B T N_m [\ln(\Lambda_m^3 \rho_m) - 1] \quad (19)$$

and

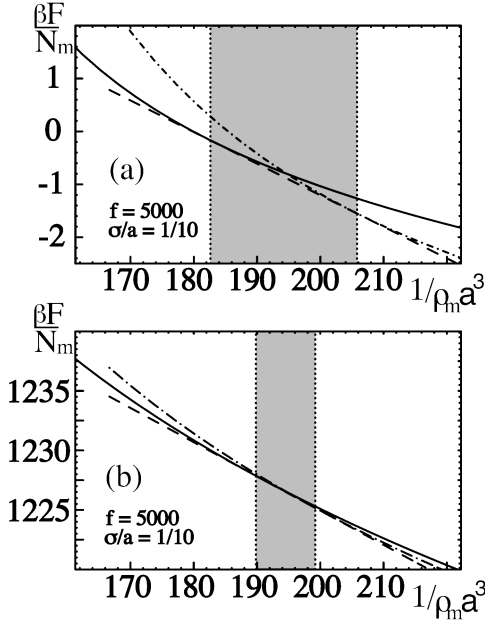


FIG. 2. Total free energy  $F/N_m$  per macroparticle in units of  $k_B T$  versus inverse macroparticle density  $1/\rho_m$  in units of  $a^3$  for the crystal phase (solid line) and the fluid phase (dot-dashed line) of the bead-spring model. The double tangent indicating the coexisting densities is shown as a dashed line. The shaded region corresponds to the density jump in the resulting phase diagram. (a) For  $f = 5000$ , and  $\sigma/a = 1/10$  without volume terms. (b) For  $f = 5000$ , and  $\sigma/a = 1/10$  with volume terms.

$$F_3^{\text{CS}} = k_B T N_m \frac{\eta_m (4 - 3\eta_m)}{(1 - \eta_m)^2}, \quad (20)$$

with  $\Lambda_m$  and  $\eta_m = \pi \rho_m d^3/6$  denoting the thermal wavelength and effective packing fraction of the macroparticles. The free energy of the *solid* is approximated by a cell approach for the hard-sphere crystal as used in [24] which is explicitly given by

$$F_3 \equiv F_3^s = k_B T N_m \left\{ -\ln \left[ \frac{\Lambda_m^{-3}}{\sqrt{2}} \left( \frac{2^{1/6}}{\rho_m^{1/3}} - d \right)^3 \right] - C \right\}, \quad (21)$$

with  $C = 2.1$ .

Results for the total free energy per macroparticle,  $F/N_m$ , in the fluid and solid phases are shown in Figs. 2 and 3 versus inverse core density  $1/\rho_m$  for different parameters  $f$  and  $\sigma/a$ . First, as a reference case, we have shown the result where all additional volume terms are neglected and the effective potential  $V(R)$  alone is used to compute the coexisting densities [Figs. 2(a) and 3(a)]. Phase coexistence is obtained by the familiar double tangent construction. One clearly sees that the large density jump is strongly reduced if the volume terms are taken into account as shown in Figs. 2(b) and 3(b). The density jump becomes smaller for an increasing number  $f$  of microscopic degrees of freedom. This can be seen by comparing Fig. 2(b) where  $f = 5000$  with Fig. 3(b) where  $f = 40\,000$ . In the latter case one can hardly see the double tangent but the phase equilibrium construction becomes visible when subtracting the linear part of the free

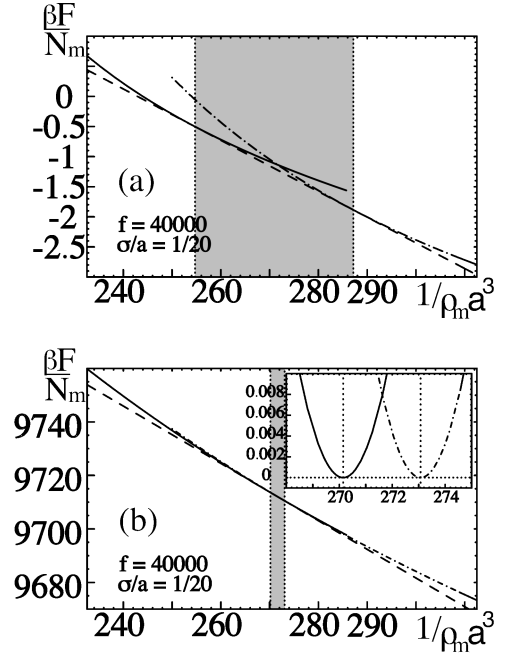


FIG. 3. Same as Fig. 2 but now for a higher number of microscopic degrees of freedom  $f = 40\,000$ , and  $\sigma/a = 1/20$ . The inset of (b) shows the free energy  $F/N_m$  per macroparticle in units of  $k_B T$  versus inverse macroparticle density  $1/\rho_m$  with the linear double tangent subtracted.

energy as shown in the inset. Hence, for large  $f$ , the phase transition occurs when the fluid and solid energies cross and it is practically *isochoric*.

For the sake of completeness we have also plotted the effective potentials belonging to the parameters of Figs. 2 and 3 together with their effective diameter  $d$  in Fig. 4. Since the potential  $V(R)$  becomes steeply repulsive at  $R \approx d$ , the mapping onto an effective hard-sphere system is justified.

### III. STAR POLYMERS

Star polymers consist of a number of  $f$  polymer chains attached to a central microscopic core. The bead-spring model of the preceding section is only a crude model of star polymers since one arm has only one degree of freedom and behaves as a single spring. In this section we extend our

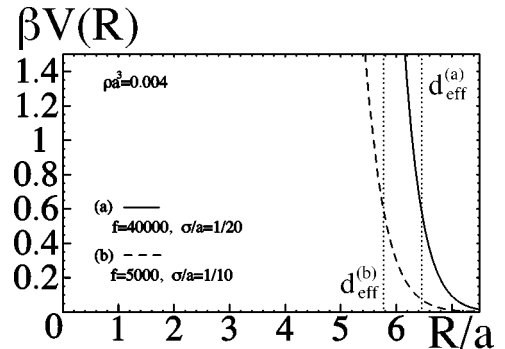


FIG. 4. Effective potential  $V(R)$  in units of  $k_B T$  versus reduced separation  $R/a$  together with the effective hard-core diameter  $d$ . (a) For  $\rho a^3 = 0.004$ ,  $f = 40\,000$ , and  $\sigma/a = 1/20$ . (b) For  $\rho a^3 = 0.004$ ,  $f = 5000$ , and  $\sigma/a = 1/10$ .

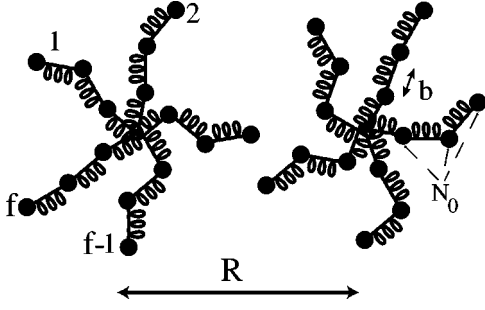


FIG. 5. Schematic picture of the star polymer model used.  $f$  Gaussian chains each of which consists of  $N_0$  monomers with a mutual average distance  $b$  are attached to a core. The core-core separation between a pair of star polymers is  $R$ .

previous analysis to a slightly more complicated model where the arms of the star are modeled by a Gaussian chain [25], see Fig. 5. The excluded volume of the chain is then treated perturbatively. Hence our analysis should apply close to the  $\Theta$  point of a star polymer solution. In the model, one chain carries  $N_0$  monomers which possess a mutual average microscopic distance  $b$ . Typically  $N_0 \approx O(10^2 - 10^5)$  while  $f$  can be of order 3–300. Note that the bead-spring model of Sec. II can be considered as a special case of the Gaussian chain model where  $N_0 = 1$ .

The total monomer density  $\phi(r)$  around the fixed core at the origin is given by a superposition of Gaussians [25]:

$$\phi(r) = \sum_{n=1}^{N_0} f \left( \frac{3}{2\pi b^2 n} \right)^{3/2} \exp\left(-\frac{3r^2}{2nb^2}\right). \quad (22)$$

In the continuum limit  $\sum_{n=1}^{N_0} \dots \rightarrow \int_1^{N_0} dn \dots$  this reads

$$\phi(r) = \frac{3}{2} \frac{f}{\pi b^2 r} \left[ \Phi\left(\sqrt{\frac{3}{2}} \frac{r}{b}\right) - \Phi\left(\sqrt{\frac{3}{2N_0}} \frac{r}{b}\right) \right], \quad (23)$$

where  $\Phi(x) = (2/\sqrt{\pi}) \int_0^x dy \exp(-y^2)$  is the probability integral. For large distances  $r$  from the cores the leading term in  $\phi(r)$  behaves as  $\propto \exp(-3r^2/2b^2N_0)/r^2$  which falls off slightly faster than the pure Gaussian profile known from the preceding section. The typical extension of the monomer density around a single star is given by the radius of gyration  $R_g$  which is related to the second moment of  $\phi(r)$ :

$$R_g^2 := \frac{\int_V d^3r r^2 \phi(r)}{\int_V d^3r \phi(r)} = \frac{N_0 + 1}{2} b^2. \quad (24)$$

Taking now into account the interaction between the monomers modeled as hard spheres with a microscopic diameter  $\sigma$ , one follows the same strategy as in the preceding section [25]. We then obtain the effective potential between two star polymer centers to be

$$V(R) = \frac{18}{\pi^2} \frac{f^2}{b^4 R} \frac{d^2 \Psi(\bar{\rho})}{d\rho^2} \left[ I\left(R, \frac{b^2}{3}\right) + I\left(R, \frac{b^2 N_0}{3}\right) - 2I\left(R, \frac{b^2}{6}(N_0 + 1)\right) \right], \quad (25)$$

where  $\bar{\rho} = fN_0\rho_m$  is the mean monomer density,  $\rho_m$  denoting the number density of the cores, and the function  $I(R, \alpha^2)$  is analytically given by

$$I(R, \alpha^2) = \frac{\pi R^2}{4} \left[ 1 - \Phi\left(\frac{R}{2\alpha}\right) \right] - \frac{\pi \alpha^2}{2} \Phi\left(\frac{R}{2\alpha}\right) - \frac{\sqrt{\pi} R \alpha}{2} \exp(-R^2/4\alpha^2) \quad (\alpha > 0). \quad (26)$$

The large distance behavior for the effective potential is governed by

$$V(R) \approx \exp\left(-\frac{3R^2}{4b^2 N_0}\right) / R^4 \quad (27)$$

decaying faster than the pure Gaussian potential from the preceding section.

All the volume terms are now summarized by

$$F_1 = F_{\text{single}} N_m + \Psi(\bar{\rho}) \mathcal{V} - \frac{1}{2} \frac{d^2 \Psi(\bar{\rho})}{d\rho^2} \bar{\rho}^2 \mathcal{V} + \frac{d^2 \Psi(\bar{\rho})}{d\rho^2} f \left( \frac{3}{\pi b^2} \right)^{3/2} [\sqrt{2N_0 + 2} - \sqrt{N_0 - 1}] / N_0 \bar{\rho} \mathcal{V}, \quad (28)$$

where  $F_{\text{single}}$ , the entropy for a single star, is irrelevant for the phase boundary analysis.

Proceeding with the same hard-sphere mapping as in Sec. II C we obtain the phase boundaries for the freezing transition. Results are shown in Fig. 6(a) where we plotted the coexisting fluid and solid densities versus the arm number  $f$  for two values of  $N_0$ . If the density is scaled with the inverse cube of the radius of gyration  $R_g$  the phase boundaries are insensitive to  $N_0$  but sensitive to  $f$ . The relative density jump  $(\rho_s - \rho_f)/\rho_f$  is shown versus  $f$  in Fig. 6(b). It can be seen that this jump strongly depends on  $f$ : while it is more than 10% for small arm numbers ( $f \approx 5$ ), it is strongly reduced for large arm numbers ( $f \approx 200$ ). If one would neglect the volume terms, the density jump would be practically constant, i.e., independent of  $f$  and  $N_0$ . This is also shown in Fig. 6(b).

## IV. CHARGED COLLOIDAL SUSPENSIONS

### A. Density-functional perturbation theory of the effective interaction

We now turn to charged colloidal suspensions and derive the effective pair potential between the macroions in a similar way as before. Again additional ‘‘volume terms’’ show up in the total free energy which have to be taken into account when exploring the phase boundaries. To obtain the effective interaction of charged colloids we start from the primitive model [26], assuming that the macroions, counterions, and salt ions are point charges, carrying charges  $Ze$ ,  $qe$ , and  $\pm qe$ , respectively. The solvent is described by a uniform background of dielectric constant  $\epsilon$ . The macroion number density is  $\rho_m = N_m/V$ , and the system is held at fixed temperature  $T$ . We further assumed that the counterions and all salt ions have the same valency and that equally charged microscopic ions are indistinguishable. Similar calculations

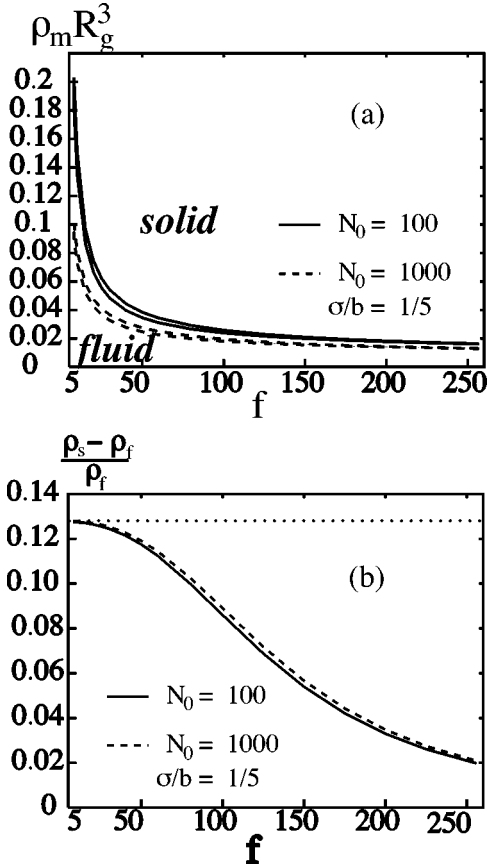


FIG. 6. (a) Phase boundaries for the freezing transition in the star polymer model. The coexisting densities in units of  $1/R_g^3$  for the fluid and solid phase are shown versus arm number  $f$  for  $N_0 = 100$  (solid line) and  $N_0 = 1000$  (dashed line). The coexistence region is shown by the shaded area. The ratio  $\sigma/b$  is  $1/5$ . (b) Relative density jump  $(\rho_s - \rho_f)/\rho_f$  versus arm number  $f$  for the star polymer model:  $N_0 = 100$  (solid line), and  $N_0 = 1000$  (dashed line). The dotted line is the result without taking the volume terms into account. The ratio  $\sigma/b$  is  $1/5$ .

including also the finite macroion core have been recently published by van Roij and Hansen [15].

### 1. Salt-free case

Let us first focus on the salt-free case, where the solution consists only of macroions and counterions. Global charge neutrality connects the number of macroions  $N_m$  with the number of counterions  $N_c$ . Integrating out the counterion degrees of freedom formally leads to an effective Hamiltonian [27,26]

$$\mathcal{H}_{\text{eff}} = K_m + V_m + \mathcal{F}_c(T, [\rho], \{\vec{R}_1, \dots, \vec{R}_{N_m}\}), \quad (29)$$

consisting of the kinetic energy of the macroions  $K_m$ , the Coulomb interaction energy between the macroions  $V_m$ , and the free energy of an inhomogeneous one-component plasma describing the counterions in the field of the macroparticles at positions  $\vec{R}_i$  ( $i = 1, \dots, N_m$ ).

The counterion free energy  $\mathcal{F}_c(T, [\rho], \{\vec{R}_1, \dots, \vec{R}_{N_m}\})$  can be expressed as a functional of the counterion one-particle density field  $\rho(\vec{r})$  which becomes minimal for the equilibrium density field under the constraint of fixed aver-

age counterion density  $(1/V) \int_V \rho(\vec{r}) = \bar{\rho} \equiv (-Z/q) \rho_m$ . It can be split into three parts as follows:

$$\mathcal{F}_c = \mathcal{F}_c^{\text{id}} + \mathcal{F}_c^{\text{MF}} + \mathcal{F}_c^{\text{ext}}.$$

Here the nonlinear but local ideal term is given by

$$\mathcal{F}_c^{\text{id}} = k_B T \int_V d^3 r \rho(\vec{r}) \{ \ln[\Lambda^3 \rho(\vec{r})] - 1 \}.$$

All counterion correlations are approximately contained in the mean-field term

$$\mathcal{F}_c^{\text{MF}} = \frac{1}{2} \int_V d^3 r \int_V d^3 r' \rho(\vec{r}) \rho(\vec{r}') \frac{q^2 e^2}{\epsilon} \frac{1}{|\vec{r} - \vec{r}'|}$$

and the coupling to the macroion coordinates is described by

$$\mathcal{F}_c^{\text{ext}} = \int_V d^3 r \rho(\vec{r}) \sum_{i=1}^{N_m} \frac{Z q e^2}{\epsilon} \frac{1}{|\vec{r} - \vec{R}_i|}.$$

We now quadratically expand the nonlinear ideal term around the mean counterion density  $\bar{\rho}$ :

$$\begin{aligned} \mathcal{F}_c^{\text{id}} \approx & F^0 + k_B T \int_V d^3 r \ln(\Lambda^3 \bar{\rho}) [\rho(\vec{r}) - \bar{\rho}] \\ & + k_B T \int_V d^3 r \frac{1}{2\bar{\rho}} [\rho(\vec{r}) - \bar{\rho}]^2, \end{aligned}$$

with

$$F^0 = N_c k_B T [\ln(\Lambda^3 \bar{\rho}) - 1],$$

which is the free energy of an ideal gas of counterions. Now the minimization of  $\mathcal{F}_c(T, [\rho], \{\vec{R}_1, \dots, \vec{R}_{N_m}\})$  with respect to  $\rho(\vec{r})$  can be done analytically [28] leading to the equilibrium density

$$\rho(\vec{r}) = \left| \frac{Z}{q} \right| \frac{\kappa^2}{4\pi} \sum_{i=1}^{N_m} \frac{e^{-\kappa|\vec{r} - \vec{R}_i|}}{|\vec{r} - \vec{R}_i|},$$

where  $\kappa = \sqrt{4\pi(q^2 e^2 / \epsilon k_B T) \bar{\rho}}$  is the inverse Debye screening length.

Inserting this density profile in the free energy functional leads to an effective Hamiltonian

$$\mathcal{H}_{\text{eff}} = K_m + V_{\text{pot}} + F^0 + F^1,$$

where

$$V_{\text{pot}} = \sum_{\substack{i,j \\ i < j}}^{N_m} V^{\text{DLVO}}(|\vec{R}_i - \vec{R}_j|) \equiv \sum_{\substack{i,j \\ i < j}}^{N_m} \frac{Z^2 e^2}{\epsilon} \frac{e^{-\kappa|\vec{R}_j - \vec{R}_i|}}{|\vec{R}_j - \vec{R}_i|}$$

is the total potential energy from the usual Derjaguin-Landau-Verwey-Overbeek (DLVO) pair interaction [2,5]. There are two ‘‘volume terms:’’  $F^0$  and

$$F^1 = -\frac{1}{2} \left( N_m \frac{Z^2 e^2}{\epsilon} \kappa + k_B T N_c \right),$$

which involves the coupling to the macroions as well as correlational contributions.

## 2. Case of added salt

In this case we have the salt concentration as an additional parameter. The total mean number density of counterions and cations is denoted with  $\bar{\rho}_+ = N_+/V$ , whereas the coions (carrying a charge  $-qe$ ) have a mean density  $\bar{\rho}_- = N_-/V$ .

Again the density-functional language can be applied involving ideal terms for the counterions and coions as well as the mean-field term describing the Coulomb coupling [28,29]. The free energy functional of the small ions is approximated by an ideal gas term

$$\mathcal{F}_c^{\text{id}} = k_B T \sum_j \int_{\mathcal{V}} d^3 \vec{r} \rho_j(\vec{r}) \{ \ln[\Lambda^3 \rho_j(\vec{r})] - 1 \},$$

where the summation takes into account positive and negative ions  $j = (+, -)$ , a mean-field contribution

$$\mathcal{F}_c^{\text{MF}} = \frac{1}{2} \sum_{j,j'} \int_{\mathcal{V}} d^3 \vec{r} \int_{\mathcal{V}} d^3 \vec{r}' \rho_j(\vec{r}) \rho_{j'}(\vec{r}') \frac{q^2 e^2}{\epsilon} \frac{1}{|\vec{r} - \vec{r}'|}$$

and the term describing the ions in the external field of the macroions

$$\mathcal{F}_c^{\text{ext}} = \sum_j \int_{\mathcal{V}} d^3 \vec{r} \rho_j(\vec{r}) \sum_{i=1}^{N_m} \frac{Z q e^2}{\epsilon} \frac{1}{|\vec{r} - \vec{R}_i|}.$$

Doing a similar analysis as in the preceding section, one obtains the following equilibrium densities for the counterions and coions:

$$\rho_+(\vec{r}) = \left( -\frac{Z}{q} \right) \frac{\kappa_+^2}{4\pi} \sum_{i=1}^{N_m} \frac{e^{-\kappa_+ |\vec{r} - \vec{R}_i|}}{|\vec{r} - \vec{R}_i|} + \frac{2\bar{\rho}_+ \bar{\rho}_-}{\bar{\rho}_+ + \bar{\rho}_-}$$

and

$$\rho_-(\vec{r}) = \left( \frac{Z}{q} \right) \frac{\kappa_-^2}{4\pi} \sum_{i=1}^{N_m} \frac{e^{-\kappa_- |\vec{r} - \vec{R}_i|}}{|\vec{r} - \vec{R}_i|} + \frac{2\bar{\rho}_+ \bar{\rho}_-}{\bar{\rho}_+ + \bar{\rho}_-},$$

where  $\kappa = \sqrt{\kappa_+^2 + \kappa_-^2}$  is the inverse Debye screening length with  $\kappa_{\pm}^2 = 4\pi(q^2 e^2 / \epsilon k_B T) \bar{\rho}_{\pm}$ .

Inserting these density profiles in the free energy functional leads again to the usual DLVO pair interaction between the macroparticles  $V^{\text{DLVO}}(R) = (Z^2 e^2 / \epsilon) (e^{-\kappa R} / R)$ . The effective Hamiltonian now involves three ‘‘volume terms,’’ namely,

$$F_+^0 = N_+ k_B T [ \ln(\Lambda^3 \bar{\rho}_+) - 1 ],$$

$$F_-^0 = N_- k_B T [ \ln(\Lambda^3 \bar{\rho}_-) - 1 ],$$

and

$$F^1 = -\frac{1}{2} \left[ N_m \frac{Z^2 e^2}{\epsilon} \kappa + k_B T (N_+ - N_-) \left( \frac{\bar{\rho}_+ - \bar{\rho}_-}{\bar{\rho}_+ + \bar{\rho}_-} \right) \right].$$

## B. The freezing transition of charged colloids

### 1. Macroionic free energies in the fluid and solid phases

Canonically averaging over the macroparticle degrees of freedom leads to a total free energy

$$F = F_m + F^0 + F^1,$$

where  $F_m$  is the free energy of a one-component system of macroparticles interacting by the effective pair potential  $V^{\text{DLVO}}(R)$ . We divide  $V^{\text{DLVO}}(R)$  into a short-range reference part  $V_0(R)$  and a long-range perturbation part  $W(R)$  such that  $V^{\text{DLVO}}(R) = V_0(R) + W(R)$ , following the scheme of Kang *et al.* [30]:

$$V_0(R) = \begin{cases} V^{\text{DLVO}}(R) - F(R) & \text{for } R < R_0 \\ 0 & \text{for } R \geq R_0 \end{cases}$$

and

$$W(R) = \begin{cases} F(R) & \text{for } R < R_0 \\ V^{\text{DLVO}}(R) & \text{for } R \geq R_0. \end{cases}$$

The splitting distance  $R_0$  is the nearest neighbor lattice distance  $R_0 = \sqrt{3}/2(2/\rho)^{1/3}$  of a bcc solid.  $F(R)$  is assumed to be a linear function  $F(R) \equiv a + bR$ , where the constants  $a$  and  $b$  are determined by requiring  $V_0(R)$  and  $W(R)$  and their derivatives to be continuous at  $R = R_0$ . The short-range potential  $V_0(R)$  is then further approximated by a hard-sphere interaction with an effective diameter  $d$  according to the Barker-Henderson formula (17)

$$d = \int_0^{R_0} dR [1 - e^{-\beta V_0(R)}]. \quad (30)$$

In the *fluid* phase the free energy of the hard-sphere reference system is obtained as in Sec. II C with the help of the Carnahan-Starling expression. In addition to that we add the free energy  $F_{\text{pert}}^f$  associated with  $W(R)$  perturbatively as

$$\frac{\beta F_{\text{pert}}^f}{N_m} = \frac{1}{2} \rho_m \int d^3 R g_0(R) \beta W(R), \quad (31)$$

where  $g_0(R)$  is the radial distribution function of the hard-sphere fluid which is analytically available, e.g., in the Verlet-Weis treatment [21].

For high densities, the system is expected to freeze into a *bcc-solid* phase. Similar to Eq. (21), we use a free volume theory [31] to obtain the free energy of a bcc hard-sphere solid

$$\frac{\beta F^s}{N_m} = -\ln \left\{ \Lambda_m^{-3} 1/2 \left[ \left( \frac{2}{\rho_m} \right)^{1/3} - d_{\text{eff}} \right]^3 \right\} - C, \quad (32)$$

with  $C = 2.1$  and add a lattice sum [32] to get the free energy  $F_{\text{pert}}^s$  associated with  $W(R)$  in the solid phase

$$F_{\text{pert}}^s = \frac{1}{2} N_m \sum_{R_{nkl}} W(\vec{R}_{nkl}), \quad (33)$$

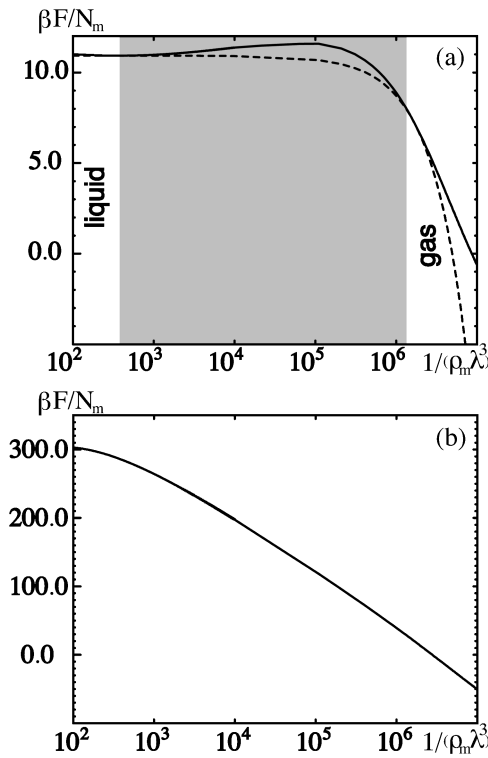


FIG. 7. Same as Fig. 2 but now for charged colloids interacting via the DLVO pair potential: Total free energy  $F/N_m$  per macroparticle in units of  $k_B T$  versus inverse colloidal particle density  $1/\rho_m$  in units of the Bjerrum length  $\lambda^3$  ( $\lambda \equiv e^2/\epsilon k_B T$ ). The parameters are  $Z=35$ ,  $T=298\text{K}$ ,  $\epsilon=81$ . Note the logarithmic scale in the inverse density. (a) Without volume terms. Here an artificial liquid-gas phase coexistence is observed (shaded area). The double tangent is the broken line. Note that due to the semi-logarithmic inverse-density axis, the double tangent is no longer linear. (b) With volume terms. There is no liquid-gas phase transition.

where the summation runs over the bcc-lattice positions  $\vec{R}_{nkl}$ . We have also considered the case of a fcc solid with a similar route to get its free energy as in Sec. II C.

## 2. Results

If the “volume terms” are omitted in the salt-free case, a “pure” one-component system governed by the DLVO potential exhibits a gas-liquid phase transition although there are no attractive interactions [16]. The reason for that is that the screening parameter  $\kappa$  depends on density. Within our theoretical approach, the results with a gas-liquid phase transition of the “pure” one-component system are shown in Fig. 7(a). This transition is spurious, however, since it disappears if the “volume terms” are added to the free energy which is shown in Fig. 7(b). This strikingly demonstrates the importance of the volume terms in locating phase boundaries. Conversely it can happen that the volume terms drive a new liquid-gas transition which is absent for the “pure” one-component system. This was investigated in more detail by van Roij and Hansen [15].

In the salt-free case, when all counterions stem from the macroions, phase equilibrium between the solid phase and the fluid phase of the macroparticles is obtained by the equilibrium of the total pressure in both phases as well as the

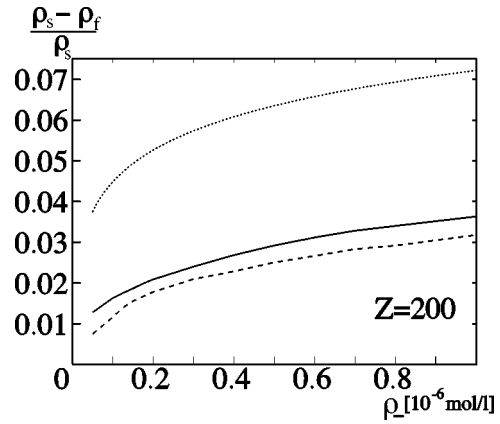


FIG. 8. The relative density jump  $(\rho_s - \rho_f)/\rho_s$  with  $\rho_s$  denoting the macroionic density of the bcc solid phase and  $\rho_f$  denoting that of the coexisting fluid phase versus the concentration  $\rho_-$  of added salt is shown. Units of  $\rho_-$  are micromoles per liter. The macroion charge is  $Z=200$ . The other parameters are given in the text.

equilibrium of the chemical potential of the macroparticles. Global charge neutrality then causes equalization of the chemical potential of the counterions in both phases. However, when adding salt one has to fulfill additionally the equality the chemical potential of the salt ions. This leads to a higher salt concentration in the fluid phase.

When calculating the phase boundaries one may follow three different routes. First, one can directly map the system onto a state-independent Yukawa system and take the phase boundaries from this system as was done by Monovoukas and Gast [7]. This approach neglects the density dependence of the inverse Debye screening length  $\kappa$  across the phase transition. Second, one can include this but neglect the volume terms. The correct way is—thirdly—to include these volume terms as well in the phase coexistence analysis. It is worth noting that the phase boundaries themselves are practically equal and not affected by the procedure used. More details, however, such as the relative density jump across the phase transition, are heavily affected by the procedure. This is strikingly shown in Fig. 8 where we show the relative density jump for charged colloids versus salt concentration. The parameters are  $Z=200$ ,  $q=1$ ,  $\epsilon=81$ , and  $T=298\text{K}$ . The pure Yukawa mapping yields a density jump which is two times larger than that obtained from a state-dependent  $\kappa$ . Inclusion of the “volume terms” shrinks the relative density jump further. This reduction is particularly pronounced for strongly deionized systems where it becomes about 50%. Note that there is always a residual salt concentration of about  $0.1\ \mu\text{mol/l}$  due to the protonization of water providing a lower limit of the salt concentration.

## V. DISCUSSION AND CONCLUSIONS

In conclusion, a density jump across a phase transition in soft-matter systems can be very small if many microscopic degrees of freedom are directly coupled to the number of the macroparticles. Then the condition of constant pressure in both coexisting phases cannot be maintained for a finite density jump since the microscopic degrees of freedom dominate the osmotic pressure. In the case of star polymers the pressure was dominated by the correlational free energy of

the self-avoiding monomers while for salt-free charged suspensions the microscopic counterion entropy reduces the density jump across macroion freezing.

Let us now discuss further examples frequently encountered in soft-matter physics.

(i) *Sterically-stabilized colloids*. Colloids stabilized by grafted polymers can be viewed as star polymers with quite different length scales. While the core size in the former case is much smaller than the length of a polymer chain, it is quite the opposite for sterically stabilized suspensions such as PMMA spheres. Here the particle diameter is much larger than the thickness of the grafted polymer layer. This implies that the thermodynamics and the contribution of the grafted polymer chains to the total osmotic pressure is a *surface* contribution as compared to the macroparticle contribution. It hence can be neglected which opens the way for possible density jumps across phase transitions.

(ii) *Colloids with nonadsorbing polymers*. If one adds nonadsorbing polymers to a colloidal suspension, the effective interaction potential becomes attractive due to depletion forces, see, e.g., [33]. As in the case of added salt for charged suspensions the concentration of the polymers is not fixed by the macroparticle concentration. It hence may differ in different phases. Hence large density jumps are possible. In fact liquid-gas-like phase transitions with a huge volume jump are observed experimentally [33].

(iii) *Effects of the solvent*. One may finally worry about the influence of the discrete microscopic solvent on density jumps across phase transitions. Again the solvent concentration is not fixed by the macroparticle concentration and the ordering of the solvent near the macroparticle surfaces is a surface effect which does not contribute to the osmotic pressure.

We finally remark that the additional ‘‘volume terms’’ may bring about the occurrence of quite interesting crystalline phases that are only stable over a finite density range and are normally preempted by nonisochoric freezing. A typical situation is sketched in Fig. 9. A normal double tangent construction within the effective one-component system would exclude a metastable solid 2 phase by the nonisochoric solid 1–fluid transition. If only isochoric phase transformations are possible, the phase diagram looks quite different and the solid 2 phase becomes stable within a finite density interval. Hence it is conceivable that some unusual phases become stable for salt-free suspensions that do not show up for salted suspensions. For pair potentials that exhibit a structure on different length scales this may lead to the observability of unusual open crystalline structures or colloidal quasicrystals [34].

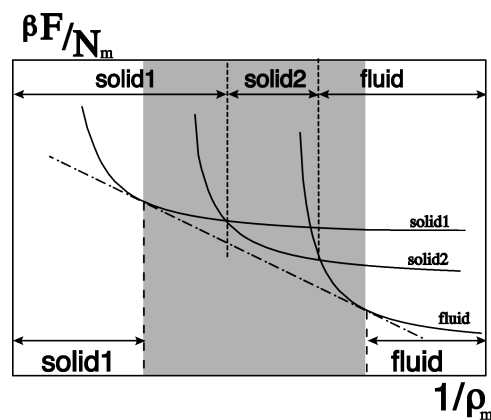


FIG. 9. Total free energy  $F/N_m$  per macroparticle versus inverse macroparticle density  $1/\rho_m$  in the case of three possible phases fluid, solid 1, and solid 2. If only the effective interaction is taken into account, the solid 2 phase is metastable and preempted by the density jump in the fluid–solid 1 transition. The corresponding double tangent is shown as a dot-dashed line and the phase diagram is sketched in the lower  $1/\rho_m$  axis. For isochoric transitions, however, as discussed in the text, the solid 2 shows up as sketched in the higher  $1/\rho_m$  axis.

To summarize: while the effective pair potential is useful to describe the static correlations as embodied in the fluid structure factor in the fluid phase one has to be careful not to forget the influence of the microscopic degrees of freedom in a discussion of the phase diagram. For a crude estimation of the phase boundaries the effective one-component pair potential picture applies reasonably well, but details as the magnitude of the density jumps across coexistence are not described correctly.

It would be interesting to resolve the magnitude of the density jumps experimentally. Using the same samples of deionized charged suspensions as discussed in Ref. [9], it should be possible to measure the density of the coexisting fluid and solid by scattering techniques, e.g., along a sedimentation profile of a charged suspension. Our consideration would lead to a practically vanishing density gap for salt-free suspensions.

#### ACKNOWLEDGMENTS

We are grateful to C. N. Likos, T. Palberg, and M. Schmidt for helpful comments. This work was supported by the DFG (Deutsche Forschungsgemeinschaft) within the Gerhard-Hess-Programm.

- [1] W. B. Russel, D. A. Saville, and W. R. Schowalter, *Colloidal Dispersions* (Cambridge University Press, Cambridge, England, 1989).  
 [2] P. N. Pusey, in *Liquids, Freezing and the Glass Transition*, edited by J. P. Hansen, D. Levesque, and J. Zinn-Justin (North-Holland, Amsterdam, 1991).  
 [3] H. Löwen, *Phys. Rep.* **237**, 249 (1994).

- [4] P. N. Pusey and W. van Meegen, *Nature (London)* **320**, 340 (1986).  
 [5] B. V. Derjaguin and L. D. Landau, *Acta Physicochim. URSS* **14**, 633 (1941); E. J. W. Verwey and J. T. G. Overbeek, *Theory of the Stability of Lyophobic Colloids* (Elsevier, Amsterdam, 1948).  
 [6] S. Alexander, P. M. Chaikin, P. Grant, G. J. Morales, P. Pin-

- cus, and D. Hone, *J. Chem. Phys.* **80**, 5776 (1984).
- [7] Y. Monovoukas and A. P. Gast, *J. Colloid Interface Sci.* **128**, 533 (1989).
- [8] M. O. Robbins, K. Kremer, and G. S. Grest, *J. Chem. Phys.* **88**, 3286 (1988).
- [9] M. Würth, J. Schwarz, F. Culis, P. Leiderer, and T. Palberg, *Phys. Rev. E* **52**, 6415 (1995).
- [10] A. P. Gast, *Langmuir* **12**, 4060 (1996).
- [11] G. S. Grest, L. J. Fetters, J. S. Huang, and D. Richter, *Adv. Chem. Phys.* **XCIV**, 67 (1996).
- [12] E. K. Lin and A. P. Gast, *Macromolecules* **29**, 390 (1996).
- [13] G. A. McConnell, A. P. Gast, J. S. Huang, and S. D. Smith, *Phys. Rev. Lett.* **71**, 2102 (1993).
- [14] G. A. McConnell and A. P. Gast, *Phys. Rev. E* **54**, 5447 (1996).
- [15] R. van Roij and J. P. Hansen, *Phys. Rev. Lett.* **79**, 3082 (1997).
- [16] M. Dijkstra and R. van Roij, *J. Phys. Condensed Matter* **10**, 1219 (1998).
- [17] E. Canessa, M. J. Grimson, and M. Silbert, *Mol. Phys.* **64**, 1195 (1988).
- [18] G. C. Barker, M. J. Grimson, and M. Silbert, *Mol. Phys.* **74**, 397 (1991).
- [19] V. Reus, L. Belloni, T. Zemb, N. Lutterbach, and H. Ver-smold, *J. Phys. II* **7**, 603 (1997).
- [20] R. Evans and M. Hasegawa, *J. Phys. C* **14**, 5225 (1981).
- [21] See, e.g., J. P. Hansen and I. R. McDonald, *Theory of Simple Liquids*, 2nd ed. (Academic Press, London, 1986).
- [22] Phase transitions within a Gaussian pair potential based on  $F_3$  alone were studied by Stillinger and co-workers [F. H. Stillinger, *J. Chem. Phys.* **65**, 3968 (1975); F. H. Stillinger and T. A. Weber, *ibid.* **68**, 3837 (1978)]. In fact, since the potential is bounded at the origin, there is an interesting reentrant melting behavior, or—equivalently—an upper critical temperature above which the system never freezes.
- [23] J. A. Barker and D. Henderson, *J. Chem. Phys.* **47**, 4714 (1967).
- [24] H. Graf, H. Löwen, and M. Schmidt, *Prog. Colloid Polym. Sci.* **104**, 177 (1997).
- [25] M. Doi and S. F. Edwards, *Theory of Polymer Dynamics* (Clarendon Press, Oxford, 1986).
- [26] H. Löwen, J. P. Hansen, and P. A. Madden, *J. Chem. Phys.* **98**, 3275 (1993).
- [27] H. Löwen, P. A. Madden, and J. P. Hansen, *Phys. Rev. Lett.* **68**, 1081 (1992).
- [28] H. Löwen, *Physica B* **220**, 78 (1996).
- [29] H. Löwen and G. Kramposthuber, *Europhys. Lett.* **23**, 673 (1993).
- [30] H. S. Kang, C. S. Lee, T. Ree, and F. H. Ree, *J. Chem. Phys.* **82**, 414 (1985).
- [31] W. W. Wood, *J. Chem. Phys.* **20**, 1334 (1952); J. G. Kirkwood, *ibid.* **18**, 380 (1950).
- [32] J. F. Lutsko and M. Baus, *J. Phys.: Condens. Matter* **3**, 6547 (1991).
- [33] S. M. Ilett, A. Orrock, W. C. K. Poon, and P. N. Pusey, *Phys. Rev. E* **51**, 1344 (1995).
- [34] A. R. Denton and H. Löwen (unpublished).